Dislocation strengthening in FCC metals and in BCC metals at high temperatures

Ronan Madec, Ladislas P. Kubin

Dislocation strengthening in FCC metals and in BCC metals at high temperatures

Ronan Madec [a], Ladislas P. Kubin [b, *]

[a] CEA, DAM, DIF, F-91297 Arpajon, France
[b] LEM, CNRS-ONERA, BP 72, 91322 Chˆatillon Cedex, France

Till now, it was widely believed that the dislocation strengthening coefficients used in the Taylor-like relation were universal for a given crystallographic class of materials. In the present study, it is shown that this is actually untrue because of two effects that influence the strength of interactions between slip systems, namely the value of the Poisson ratio and the occurrence of doubly degenerated, asymmetric, junction configurations. New strengthening coefficient values for reactions between slip systems were determined using dislocation dynamics simulations on five representative FCC metals, plus germanium, and on five BCC transition metals for {110} and {112} slip systems at high homologous temperatures. The value of the Poisson ratio affects all the strengthening coefficients to various extents ranging from small to substantial. The effects of configuration asymmetry and Poisson's ratio are more marked in BCC metals than in FCC metals. These two major effects arise from a number of concurring dislocation mechanisms, which are discussed in some detail. It is expected that the use of accurate material-dependent coefficients will notably improve the predictive ability of current models for strain hardening.

1. Introduction

The dislocation strengthening (or Taylor-like) relation, which relates the critical stress for the onset of slip to the square root of the total density, is an almost universal building block for dislocation-based models of plastic flow [1,2]. Its predictive ability was considerably enhanced when it was generalized by Franciosi et al. [3]. In this formulation, the total density is replaced by a sum of contributions containing the dislocation density of each slip system multiplied by its coefficient of interaction with other slip systems and with itself (self-interaction).

The storage-recovery model initially proposed by Kocks [4] was also generalized by Teodosiu et al. [5] in order to express the contribution of each slip system to dislocation storage and recovery. Such generalized formulations are now widely used since they can be solved using crystal plasticity finite element codes. Dislocation dynamics (DD) simulations further contributed to significantly improve their predictive ability by providing numerical values for a number of coefficients (see e.g., [6,7]). This was in particular the case for short-range reactions between non-coplanar slip systems, which essentially govern dislocation strengthening. It must be kept in mind, however, that the Taylor-like relation holds for dislocations that bow out under stress and not for straight dislocations overcoming a periodic lattice resistance. To avoid the latter case, in the present work, DD simulations were performed at the transition temperatures at which the lattice resistance vanishes.

The literature on interaction coefficients determined by DD simulations comprises several investigations on FCC metals [8–11]. The interactions of $a/2$<111>{110} slip systems were simulated without lattice friction in BCC Ta [12] and α-Fe [13] at 300 K. Interaction coefficients were also determined at room temperature in hexagonal close-packed (HCP) Mg [11], which exhibits a substantial lattice resistance on non-basal planes. Other studies were concerned with ordinary ice [14], of which the crystallographic structure is close to HCP, and MgO [15] with NaCl structure. In these last two cases, the homologous temperatures were high and the lattice resistance was negligible.

In diamond-cubic germanium, the dislocations of the glide set have the same slip geometry as FCC crystals. Alexander and Crawford [16] used a model to extract the interaction coefficients of Ge from latent hardening tests (see Ref. [17] for a review) performed at 854 K in the ductile regime. However, there is no

* Corresponding author.
E-mail addresses: ronan.madec@cea.fr (R. Madec), ladislas.kubin@onera.fr (L.P. Kubin).

published value of the elastic constants at 854 K and no value is given for the shear modulus in Ref. [16], which suggests that it was taken at room temperature. To match the way experimental results were analyzed, the DD simulations were carried out with shear moduli and Poisson's ratios taken at room temperature and without lattice friction. For this reason, and others that are discussed in Supplementary Section S1.2, these measurements must be considered as mainly semi-quantitative.

The present work is a first step in an ongoing study involving the elaboration of an accurate storage-recovery model [4,5] for FCC metals and especially BCC transition metals at high temperatures (see Section 5.2). Till now, it was assumed that the interaction coefficients were identical for all materials having the same slip geometry. The objective of the present work is to provide more accurate coefficients taking into consideration two material-dependent effects that were ignored till now. The first effect arises from an asymmetry of some junction-forming configurations, which induces a degeneracy of the related strengths. The second effect arises from the sensitivity of the coefficients to the value of the Poisson ratio.

The DD simulation method employed to determine the coefficient values is briefly recalled in Section 2. An extended set of results is presented in Section 3 for five representative FCC metals plus germanium. In BCC metals, the few available results are restricted to interactions between the $a/2<111>\{110\}$ slip systems. The modelling of the mechanical response requires, however, the knowledge of all interactions of the $a/2<111>\{110\}$ and $a/2<111>\{112\}$ slip systems. Results obtained on five representative BCC transition metals are presented in Section 4 and are complemented by the mutual interactions of {110} and {112} slip systems in Supplementary Section S5. In Section 5, the major results obtained in the present study are outlined and prospective work toward dislocation-based models for strain hardening is discussed.

2. Interaction and strengthening coefficients, DD simulations

In the generalized dislocation strengthening relation, the critical resolved shear stress for the onset of slip on slip system i, τ_c^i, is written [3].

$$\tau_c^i = \mu b \Big(\sum_j a_{ij} \rho^j \Big)^{1/2}, \tag{1}$$

where μ is an isotropic shear modulus, b is the magnitude of the Burgers vector and ρ^j is the stored dislocation density in slip system j. The summation under the square root is carried out on all slip systems. The interaction coefficients a_{ij} are dimensionless components of the so-called interaction matrix; they measure the average strength of the interaction between the primary slip systems i and other slip systems j. The strengthening coefficients $\alpha_{ij} = a_{ij}^{1/2}$ are frequently used to make comparisons between theoretical and experimental estimates [18].

As yet, the interaction strengths between coplanar slip systems (coplanar and self-interactions) cannot be measured by DD simulations for technical reasons. Reactions between dislocations gliding in non-coplanar slip systems form junctions, except in the case of annihilations of two attractive dislocations gliding in two slip planes that contain their Burgers vector (the colinear interaction, cf. [8]).

In the absence of lattice friction, dislocation reactions contribute to most of the critical stress of pure single crystals.[1] Their strength is essentially elastic in nature since it removes a significant line energy from the crystal; it is well documented in FCC metals from an extended compilation of experimental results by Basinski and Basinski [19] and several calculations (see Ref. [2] for review and discussion). At a fine scale, plastic flow is resolved into a succession of dislocation avalanches, each triggered by the unzipping of a single junction [6]. Because junction unzipping involves dislocation curvature and line tension effects, Eq. (1) contains a hidden logarithmic term, which is embedded into the interaction coefficient. The seminal study [19] showed that this term induces a dependence of the strengthening coefficients on the forest density (see also [9,18] and Supplementary Section S4.2).

At present, these large-scale DD simulations cannot be performed in anisotropic elasticity by lack of computing power. Use is made here of the Scattergood and Bacon's shear moduli and Poisson's ratios, which were shown to provide the best fit to the shape of curved dislocations [20]. Section S1 gives more detail, references on elastic stiffnesses in FCC and BCC crystals and further discusses the particular case of germanium.

The 3D simulation code used in the present study, MobiDiC, derives from the microMegas code [21]. It is constructed on similar basic principles, but incorporates an improved line model that makes it possible to treat a multiplicity of junction directions [12]. A more accurate treatment of dislocation segments ending at triple junction nodes is also implemented; it was suggested by a line tension model for junctions proposed by Dupuy and Fivel [22]. The dimensions of the elementary cells are optimized via periodic boundary conditions [23] in order to provide an isotropic slip distance of 150 μm to moving dislocations. In all cases, the volume of the elementary cell is around 10^3 μm^3.

The measurements of interaction strengths for non-coplanar slip planes were carried out using model DD simulations similar to the ones used in previous studies on FCC crystals ([9], see also Section S2). In short, primary dislocations glide under a constant applied strain rate through a constant forest density, which leads to a specific type of reaction. When the flow stress saturates the value of the strengthening coefficient under investigation can be determined. There are, however, stress fluctuations originating from dislocation avalanches [6] that constitute the major source of error. In what follows, the model simulations are carried out using a reference forest density of 10^{12} m^{-2}. The numerical results are given in terms of strengthening coefficients to facilitate the comparison with the frequently quoted strength of $\alpha = 0.35$ of the Lomer-Cottrell lock at the reference forest density [18]. A few other simulations were carried out to check the effect of changes in the forest density (Sections S4.2 and S5.3).

Fig. 1 shows an area of a model simulation on the interaction of two non-coplanar slip systems in α-iron. The mobile primary lines preferentially expand along the line direction of the junctions. This percolation effect is a quite general trend that impacts the strengthening coefficients to various extends by inducing an anisotropy of the line directions and of the related line tensions in the primary microstructure.

3. Results on FCC metals

This section discusses first two effects that were neglected till now, the effect of the Poisson ratio, which affects all materials in the Scattergood-Bacon approximation, and an asymmetry effect, which affects some particular reactions. The new coefficient values for FCC crystals at room temperature, are then tabulated and discussed.

3.1. Effect of the Poisson ratio

In most previous computations of strengthening coefficients in

[1] Long-range interactions are nevertheless computed in DD simulations.

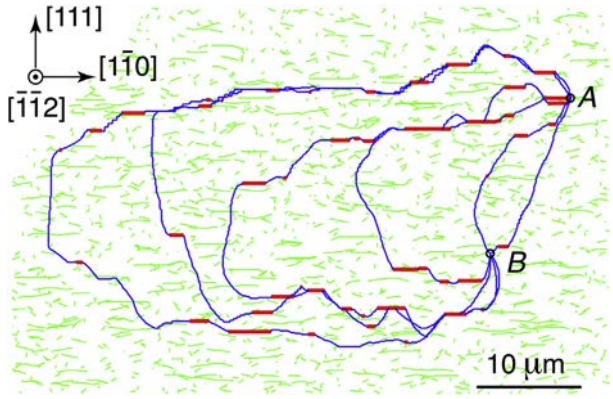

Fig. 1. Thin film parallel to the primary slip plane extracted from a model simulation in α-Fe. Snapshots of the expansion under stress of a primary $a/2[111](\bar{1}\bar{1}2)$ segment (long lines) pinned at its ends *A* and *B*, which interacts with a forest of $a/2\ [11\bar{1}](112)$ secondary trees (short wavy lines). The junctions (short and straight thick lines) are lying along the $[1\bar{1}0]$ direction of intersection of the two slip planes. They are of edge character with a Burgers vector, $\boldsymbol{b}_j = a[001]$.

FCC metals, copper was taken as a model material [8,9,11] and typical values close to $\nu = 1/3$ were used for its Poisson's ratio. However the Scattergood and Bacon approximation yields an effective Poisson's ratio of $\nu = 0.442$.

A simple way to check how the Poisson ratio affects dislocation reactions consists in mapping their domain of stability after relaxation to equilibrium. Such mappings are obtained by considering the reactions of two attractive segments of equal length crossing each other at their midpoints. The variables are the initial angles between the parent segments and the intersection of their slip planes, which contains the junction line. The angular domain of junction formation can be simulated [18,24,25] or calculated [26,27], as is done here (Fig. 2).

The stability domain of junctions is drawn from the equilibrium of line tensions at the triple nodes as determined from an energy minimization procedure (see Section S3). One obtains a central lobe duplicated by four elementary translations of $\pm\ \pi$ along the two

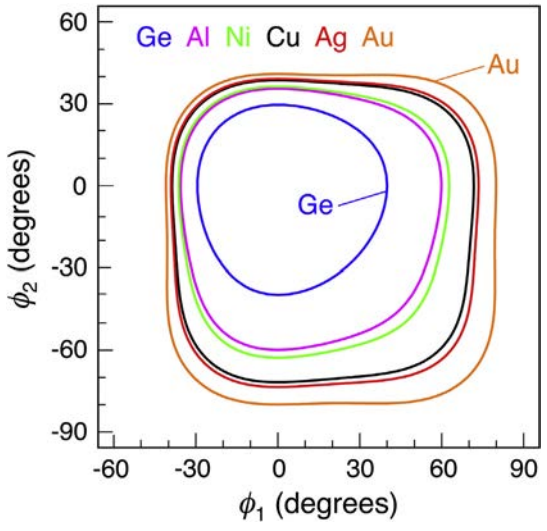

Fig. 2. Orientation mappings for the stability of the Hirth lock in Ge and representative FCC metals. The angles between the initial line directions of the interacting segments and the intersection of their slip planes are denoted by ϕ_1 and ϕ_2. The size of the central stability lobe increases with increasing Poisson's ratio, from $\nu = 0.246$ (Ge) to 0.510 (Au).

diagonals (Fig. 2). The maximal stability is obtained for the reaction of two parallel attractive dislocations at the intersection of their slip planes. Stability is by construction marginal at the periphery of the lobes.

The Hirth lock is the weakest of all reaction products. As it involves parent lines with orthogonal Burgers vectors, it is marginally stable in the constant line tension approximation. The evolution of its stability domain with increasing Poisson's ratio can be discussed as follows. There are two contributions to the energy balance of the reaction. The first one arises from the line energy removal entailed by the formation of the lock. It stabilizes the junction and increases with increasing edge component in the line energy of the parent lines. The second one arises from the energy of the lock, which has a <100> Burgers vector larger than that of its ½<110> parent segments by a factor of $\sqrt{2}$. This increases its line energy by a factor of two. In the Scattergood-Bacon approximation, the effective Poisson ratio always increases with increasing ratio of the anisotropic edge to screw pre-logarithmic energy coefficients (see Eq. S3-2). As the computations show that the first contribution prevails over the second one, the stability lobes should always expand with increasing Poisson's ratio. As illustrated by Fig. 2, the computed result is quite spectacular.

The orientation mappings are less substantially modified for the Lomer and glissile junctions (see Section S3 for a discussion). It must be noted that the strengthening coefficients cannot be estimated from these simple orientation mappings. The computed values are given in Section 3.3 and further commented.

3.2. Asymmetric interactions and coefficients

In what follows, the slip systems are labelled according to the notations of Schmid and Boas.[2] The primary slip system is that of the $[001] - [011] - [\bar{1}11]$ triangle in a [001] stereographic plot, $B4 = a/2(111)[\bar{1}01]$. A particular asymmetry effect occurs in FCC crystals, BCC crystals (Section 4) and probably in many materials with other crystallographic structures.

Consider the Burgers vectors of two initial parent segments. They make two angles with the oriented direction of intersection, which will contain the junction. Changing the sign of these angles does not change the character of the segments and does not modify their line energy and line tension (Eqs. S3-1, S3-2). Hence, the absolute values of the angles are denoted by β_i and β_j. When $\beta_i = \beta_j$, exchanging (i) and (j) does not modify the line energies involved during a reaction and one should have $\alpha_{ij} = \alpha_{ji}$. This is clearly the case for colinear annihilations ($\beta_i = 0$, $\beta_j = 0$). It can be easily verified that for the Lomer and Hirth locks the configurations are also symmetrical with $\beta_i = \beta_j = \pi/3$.

The case of the glissile junction is different. It is depicted in Fig. 3, which schematically illustrates the interaction of the primary slip system $B4 = a/2(111)[\bar{1}01]$ with the forest system $D1 = a/2(1\bar{1}1)[011]$. The junction line is formed at the intersection of planes B and D and its Burgers vector $b_j = a/2[\bar{1}10]$ is glissile in slip plane D. What matters is that its line direction, $l_j = [\bar{1}01]$, is colinear to the slip direction 4 of the primary system, so that $\beta_i = 0$. In contrast, the secondary Burgers vector, $a/2[011]$, makes an angle $\beta_j = \pi/3$ with the intersection. As the two angles differ, the strengthening coefficients for the interactions B4→D1 and D1→B4 also differ. In particular, they include different contributions of the line tension to the percolation effect (see Fig. 1 for this effect).

In what follows, asymmetric reactions are denoted respectively

[2] Schmid and Boas notations for FCC crystals. Slip planes: A = $(\bar{1}11)$, B = (111), C = $(\bar{1}\bar{1}1)$, D = $(1\bar{1}1)$. Slip directions: 1 = [011], 2 = $[0\bar{1}1]$., 3 = [101], 4 = $[\bar{1}01]$., 5 = $[\bar{1}10]$., 6 = [110].

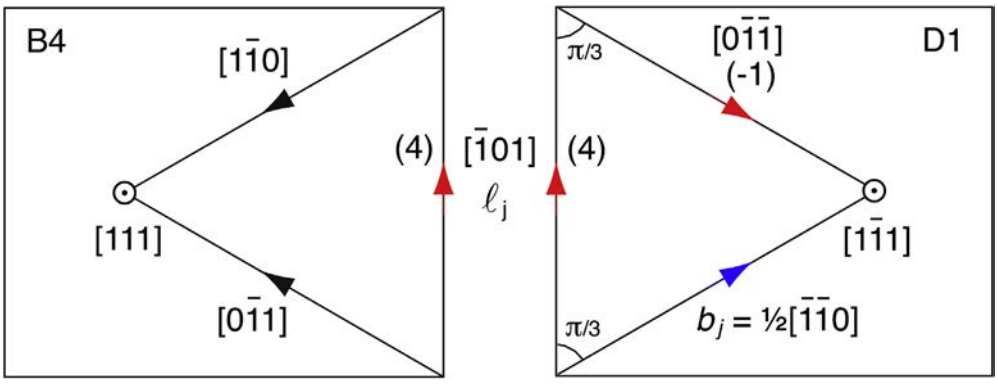

Fig. 3. An asymmetric glissile configuration. The primary slip system B4 (left) reacts with the forest system D1 (right). The Burgers vector of B4 is lying along the intersection of the two slip planes, whereas the Burgers vector 1 of slip plane D, as well as that of the junction, are making non-oriented angles of π/3 with the intersection (see text for more detail).

by $G_{0°}$ and $G_{60°}$, where G stands for 'glissile' and the indexes refer to the primary angles defined above. By reason of symmetry, such configurations occur for all glissile interactions because the intersection of the two slip planes contains one of the parent Burgers vectors but not the other one. The values of the strengthening coefficients for the glissile reactions and their type are given in the next section and further commented.

In summary, the two effects considered in the last two sections arise from differences in orientation, hence line energy. Under stress, the differences in line tensions affect in a complex manner the local junction configurations, the global percolation effect in the microstructure and the resulting critical stresses.

3.3. New coefficient values

The strengthening coefficient values drawn from model simulations are given in Table 1 for germanium, copper and other FCC metals.

The average magnitudes of the stress fluctuations caused by dislocation avalanches at saturation (Section 2) are proportional to the coefficient values. They induce a mean fluctuation of all instantaneous coefficient values, for which we take ±5% as a liberal estimate of the error. The full interaction matrix is given in Table S4-1 and the dependence of coefficient values on forest density is examined in Fig. S4-1.

Table 1
Strengthening coefficient values (within ±5%) for representative FCC crystals and germanium. The model simulations were carried out with the primary system B4 interacting with a reference forest density of 10^{12} m^{-2}. The reactions are the colinear annihilation (coli), the Hirth lock, the two glissile junctions and the Lomer lock. Values of the Poisson ratio ν and the Zener anisotropy coefficient for cubic crystals $A = 2c_{44}/(c_{11} - c_{12})$, are indicated. Note that Au exhibits the largest Poisson's ratio, $\nu = 0.51$; this high value has consequences on the segment's shapes (see Fig. S1-1 and Section S3).

B4 with Reaction	D4 Coli	A3, C3 Hirth	D1, D6 $G_{0°}$		A2, C5 $G_{60°}$	A6, C1 Lomer
	Ge	Al	Ni	Cu	Ag	Au
ν	0.246	0.363	0.381	0.442	0.455	0.510
A	1.64	1.230	2.596	3.20	2.923	2.917
coli	0.77_5	0.81	0.82	0.85	0.87	0.87_5
Hirth	0.18	0.20_5	0.21	0.23	0.23	0.24_5
$G_{0°}$	0.31_5	0.32	0.32	0.35_5	0.34	0.36
$G_{60°}$	0.29	0.30	0.30	0.295	0.31	0.31
Lomer	0.39	0.38	0.41	0.42	0.42	0.44

The collinear interaction remains by far the strongest interaction and the Hirth lock the weakest one. For some materials, there is also a substantial difference between the two coefficients for the glissile junction. The hierarchy of coefficient values undergoes, however, one modification. Whereas the glissile junction was previously found to be slightly stronger than the Lomer lock, the Lomer lock is now always stronger than the strongest glissile junction, $G_{0°}$. In copper, this is mainly due to an 18% increase of the strength of the Lomer lock with respect to previous results with $\nu = 1/3$ ([9], Table 1 of [7]).

As discussed in Section 3.1, the orientation dependence of the line energy is affected by the Poisson ratio.

Fig. 4 shows that strengthening coefficients always increase with increasing Poisson's ratio. The Hirth lock exhibits the highest relative increase (30.5%). In tension, this evolution should be rather insignificant since the weak Hirth lock is only found in the <001> orientation amidst several strong junctions. In contrast, it may matter in compression because the junction that is formed during duplex slip in stage II is not a Lomer lock but a Hirth lock.

The colinear annihilation is less affected (12%) but exhibits the largest absolute increase of all coefficients. Its line energy balance is always favourable but the 'Poisson effect' also affects the interaction strengths between the lines as well as the line tensions of the residual parent dislocations after reaction (see Section S3 for a qualitative discussion). The same considerations also explain why the Lomer lock is less sensitive to the value of the Poisson ratio than other junctions (12%), save for the $G_{60°}$ glissile junction.

The degeneracy of the glissile reaction can be understood in terms of line tension because junction unzipping requires remobilizing dislocation segments with orientations close to the percolation direction. The closer is this orientation to the screw orientation, the higher is the critical stress for primary slip, especially for high Poisson's ratio values. In the extreme cases of Au and Cu, the $G_{0°}$ junctions are 16% and 18.5% stronger than the weaker $G_{60°}$ junctions.

Although the results on germanium must be considered as semi-quantitative (Sections 1 and S1.2), the hierarchy of coefficient values determined by Alexander and Crawford [16] is the same as the one obtained here. The agreement with measured values is 5% for the Lomer lock and 6.5% for the degenerated glissile junction $G_{60°}$.[3] The agreement is less good for the glissile junction $G_{0°}$ (16%), the collinear reaction (19%) and the Hirth lock (28.5%).

[3] In this early and unique measurement, it was not noted that the two junctions were of glissile type.

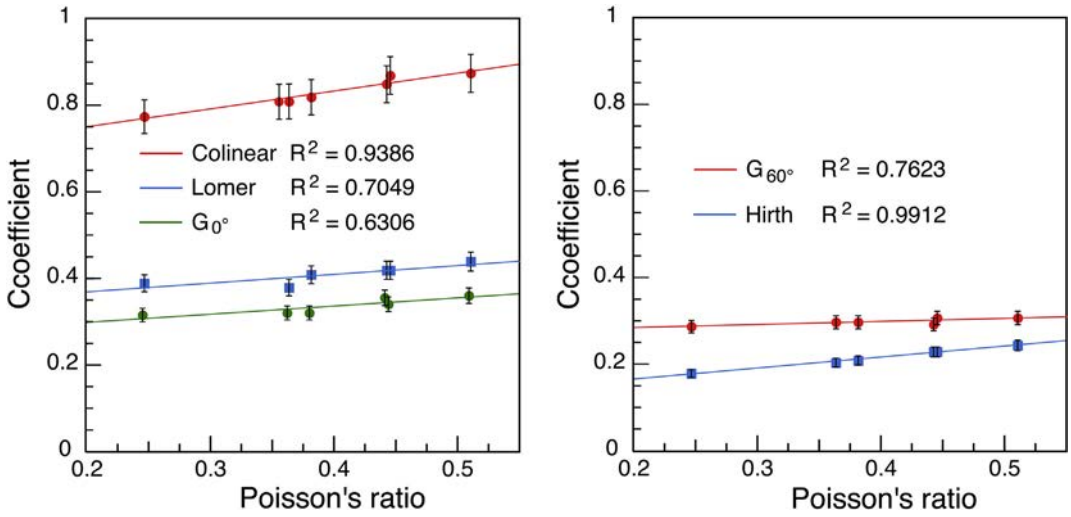

Fig. 4. Evolution of the strengthening coefficients values (within ±5%) with increasing Poisson's ratio. The linear regression lines are fits obtained by the least squares error method and R^2 is the corresponding coefficient of determination. The left figure depicts the evolution of the three strong reactions and the right one that of the two weak junctions.

4. Results on BCC metals at high temperatures

4.1. Introduction, representative BCC metals

Since the early study by Taylor and Elam on pencil glide in α-Fe [28] it is known that slip occurs not only in the primary {110} slip plane, but also by non-crystallographic wavy slip on the maximum resolved shear stress plane (MRSSP). There are few systematic investigations of slip traces in pure BCC crystals in the high temperature regime (cf. e.g. Ref. [29] for α-Fe and the detailed investigation by Richter [30] in Mo). These studies show the occurrence of slip on {112} and {123} planes, as well as of wavy slip in the MRSSP. The slip traces are found to result in Mo from 'composite slip', that is, a composition of successive slip steps of variable magnitudes on various {110} planes ([30], see also [31]). As the screw dislocation cores are very narrow in BCC metals, cross-slip should, indeed, be relatively easy in the athermal regime. As far as the modelling of BCC polycrystals in this regime is concerned, it seems impossible to take into account all the possible slip modes. Use is often made of a simplified slip geometry including only {110} and {112} slip planes [32–34]. Estimating the strengthening coefficients of {112} slip systems is, therefore, a prerequisite for assessing the predictive ability of the assumed slip geometry.

Among the present representative materials, tungsten is practically isotropic whereas α-iron has the highest Poisson ratio and Zener anisotropy coefficient. The other representative materials are Nb and Ta for column V of the periodic classification and Mo (plus W) for column VI. The transition temperatures to the athermal regime used in the present study were mostly taken from Ref. [2]. By order of increasing Poisson's ratio, they are: 465 K (Mo), 340 K (Nb), 800 K (W), 450 K (Ta) and 350 K (Fe).[4] The following sections discuss separately the values of the strengthening coefficients for {110} and {112} slip systems.

The full interaction matrix for BCC metals is given in Table S5-1, the strengthening coefficients for cross-interactions between {110} and {112} slip systems are given in Table S5-3 and the dependence of strengthening coefficients on forest density is shown in Fig. S5-2.

[4] See Section S1-2 for references to the elastic constants at these temperatures.

4.2. Notations for {110} slip systems and reactions

The notations for {110} slip systems derive from those of Schmid and Boas. As the FCC and BCC lattices are reciprocal to each other, the notations for $a/2<111>\{110\}$ slip systems are those of FCC crystals in which slip planes and slip directions are exchanged. For instance, the primary slip system in tension for FCC crystals, B4 = $a/2[\bar{1}01](111)$, is labelled B4 = $a/2[111](\bar{1}01)$ in BCC crystals.

For {110} interacting slip systems, as well as for {112} slip systems, there is a single colinear interaction with same strength in both cases. As the two interacting slip planes make an angle of 60°, it is denoted by $coli_{60°}$. In the full interaction matrix for BCC crystals (Table S5-2), there are twelve different types of junctions; they are denoted by J_i with an index i ranging from 1 to 12. For asymmetric junctions the notation is the same as in FCC metals (Section 3.2).

4.3. Strengthening coefficients for {110} slip

In BCC metals, and in contrast to FCC metals, all the junctions formed by the primary $a/2<111>$ dislocations have the same Burgers vector, $a<100>$. This Burgers vector is $2/\sqrt{3}$ times larger than the one of the primary segments, which entails a line energy increase by a factor of only 4/3. In consequence, the strength of junctions is mainly governed by the orientation dependence of the line energies. The angle between the interacting slip planes, which can take several values in BCC metals, also plays a role. This angle affects the magnitude of short-range interactions between dislocation segments; it also shifts the limit between attraction and repulsion for non-coplanar dislocation reactions.

The coefficient values for the interactions of the primary slip system B4 with other {110} slip systems are given in Table 2 for the representative BCC metals ordered by increasing Poisson's ratio. The stress fluctuations at saturation induce a mean error similar to the one estimated for FCC crystals (±5%, cf. Section 3.3).

Some features of the reaction strengths given in Table 2 can be interpreted. The colinear interaction is strengthened by increasing Poisson's ratios and, as a whole, it is somewhat stronger than in FCC crystals. This arises from the larger magnitude of the Burgers vectors ($a\sqrt{3}/2$ versus $a/\sqrt{2}$) and, consequently, of the line energy that is removed by annihilations.

The junctions are less stable than in FCC crystals because of their higher line energies, especially for low values of the Poisson ratio

Table 2
Strengthening coefficient values (within ±5%) for representative BCC crystals. The primary slip system B4 = $a/2[111](\bar{1}01)$ interacts with other {110} slip systems. There is one colinear annihilation (coli$_{60°}$) and four junctions, two asymmetric ones ($J_{1\ 0°}$ and $J_{1\ 70°53'}$) and two symmetric ones (J_2 is edge and J_3 has a mixed character). The values of the Poisson ratio ν and of the Zener anisotropy coefficient A are indicated. The model simulations were carried out with a reference forest density of 10^{12} m^{-2}. The transition temperatures to the athermal regime are given in Section 4.1.

B4 with Reaction	B2, B5 coli $_{60°}$	A2, C5 $J_{1\ 0°}$	D6, D1 $J_{1\ 70°53'}$	A3, C3 J_2	A6, C1 J_3
	Mo	Nb	W	Ta	Fe
ν	0.221	0.257	0.296	0.430	0.478
A	0.730	0.499	1.044	1.575	2.439
coli $_{60°}$	0.790	0.82_5	0.800	0.88	0.93
$J_{1\ 0°}$	0.25	0.24_5	0.25	0.27_5	0.29_5
$J_{1\ 70°53'}$	0.20	0.20_5	0.21	0.20_5	0.19_5
J_2	0.30_5	0.310	0.32	0.34_5	0.34
J_3	0.25	0.28_5	0.30	0.35	0.39

Table 3
Strengthening coefficient values (within ±5%) for representative BCC crystals. The primary slip system B$\underline{3}$ = $a/2[111](\bar{2}11)$ interacts with other {112} slip systems. There is one colinear annihilation (coli $_{60°}$) and five junctions, two asymmetric ones ($J_{10\ 28°56'}$ and $J_{10\ 72°98'}$) and three symmetric ones with edge (J_9 and J_{12}) and mixed (J_{11}) character. The values of the Poisson ratio ν and of the Zener anisotropy coefficient A are the same as in Table 2. The model simulations were carried out with a reference forest density of 10^{12} m^{-2}. The transition temperatures to the athermal regime are given in Section 4.1.

B$\underline{3}$ with Reaction	B$\underline{7}$, B$\underline{12}$ coli $_{60°}$	A$\underline{4}$ J_9	A$\underline{8}$, A$\underline{11}$ $J_{10\ 28°56'}$	C$\underline{2}$, D$\underline{6}$ $J_{10\ 72°98'}$	C$\underline{5}$ J_{11}	B$\underline{7}$, C$\underline{2}$ J_{12}
	Mo	Nb	W	Ta	Fe	
ν	0.221	0.257	0.296	0.430	0.478	
A	0.730	0.499	1.044	1.575	2.439	
coli $_{60°}$	0.790	0.82_5	0.800	0.88	0.93	
J_9	0.23_5	0.28	0.29	0.34_5	0.35_5	
$J_{10\ 28°56'}$	0.21_5	0.23_5	0.22	0.26	0.28_5	
$J_{10\ 72°98'}$	0.19_5	0.23	0.24	0.25_5	0.26	
J_{11}	0.26	0.26_5	0.27_5	0.37	0.37	
J_{12}	0.20	0.19	0.17	0.16_5	0.15	

(see e.g., the junction $J_{1\ 70°53'}$ of Mo). The strength variations originate from the mechanisms mentioned above and, in addition, from the impact on the line tension of the microstructural anisotropy induced by the percolation of dislocations along the junction direction (Fig. 1). By comparison with the Lomer and glissile junctions, it appears that all these effects result in a less uniform behaviour of the coefficients with increasing Poisson's ratio. For example, the edge junction J_2 is slightly strengthened, as illustrated by its stability lobe (Fig. S3-2a). In contrast, the strength of the junction $J_{1\ 70°53'}$ remains rather stable whereas the mixed symmetric junction J_3, which is the second weakest junction for Mo, becomes the strongest one for α-iron. The properties of junctions are also semi-quantitatively discussed in Section S3.2 from the related stability lobes (Fig. S3-2).

Like in FCC crystals, the difference in strength between the asymmetric junction with a primary screw along the junction direction ($J_{1\ 0°}$) and its counterpart ($J_{1\ 70°53'}$) is affected by the anisotropy of the microstructure; it increases with increasing Poisson's ratio.

4.4. Strengthening coefficients for {112} slip systems

For {112} slip systems, the notations for the Burgers vectors are unchanged and the labelling of the {112} slip planes is usually taken from the numbering devised by Schmid and Boas for twinning systems (Fig. 11 of [35], Fig. 1 of [36], see Fig. S5-1).[5] As for {110} slip systems, the labelling of {112} slip systems follows the order of Burgers vectors and, for each of them, it follows the order of slip planes as given in the notation for twinning systems [37].

Table 3 gives the values of the interaction coefficients of the primary {112} slip system B$\underline{3}$ = a/2[111]$(\bar{2}11)$, which is activated in the right part of the standard stereographic triangle, with other {112} slip systems. In the Scattergood and Bacon approximation, the shear moduli and effective Poisson's ratios are identical to those of {110} slip (Section S1.1). The errors in coefficient values are similar to the ones recorded for FCC crystals and {110} slip in BCC crystals.

The mechanisms governing the reaction strengths shown in Table 3 are the same as in {110} slip (Section 4.3). The collinear interaction has same geometry as the one formed in {110} slip and exhibits the same strength. In the case of the asymmetric J_{10} junction, the combined effect of asymmetry and Poisson's ratio is less pronounced than in {110} slip because the junction direction is of mixed character regardless of its primary slip system. For symmetrical junctions the effect of increasing Poisson's ratio is, again, of variable sense and magnitude. For example, the edge junction J_9 is strongly strengthened because its energy and those of its two parent segments evolve in the same manner, which increases the energy gain of the reaction. For the opposite reason, that is, because of line energies evolving in a different manner, the edge junction J_{12} is only slightly softened.

The character of the junctions also plays a role. The mixed junction J_{11} is substantially stronger than other junctions and nearly as strong as the mixed junction J_3 in {011} slip because its character is the closest to screw orientation. Its line energy increases less than the one of its parent segments (see Fig. S3-2c and the discussion of stability lobes in Section S3).

As a consequence of all these effects, the evolution of junction strengths with increasing Poisson's ratio is far from being uniform (see Table 3). For instance, the strength of junctions J_9 and J_{11} substantially increases, whereas the ones of J_{10} moderately increase and the one of J_{12} slightly decreases. Such large differences do not occur in {110} slip.

Most of the trends mentioned above are also observed for the mutual interactions between {110} and {112} systems (Table S5-3). In that case there are five junctions, which are all doubly degenerated. Thus, among the twelve different types of junctions formed in BCC metals, seven are doubly degenerated (Table S5-2).

5. Concluding remarks

The determination of the strengthening coefficients for reactions between slip systems allows one to remove a number of free parameters from dislocation-based models for strain hardening. Till now, it was widely believed that these coefficients were universal for a given crystallographic class of materials. As shown in the present study, that is actually not true because of two effects that influence the interaction strengths, namely the effect of the Poisson ratio and the occurrence of asymmetric, doubly degenerated junction configurations.

New strengthening coefficient values were determined using DD simulations on five representative FCC metals at 300 K, plus germanium, and of five representative BCC transition metals at high homologous temperatures. A wealth of more or less complex mechanisms were found to govern the strengths of dislocation

[5] Notations for {112} slip in BCC crystals after Fig. S5-1: $\underline{1} = (\bar{1}12)$, $\underline{2} = (112)$, $\underline{3} = (\bar{2}11)$, $\underline{4} = (211)$, $\underline{5} = (\bar{1}21)$, $\underline{6} = (121)$, $\underline{7} = (\bar{1}\bar{1}2)$, $\underline{8} = (1\bar{1}2)$, $\underline{9} = (\bar{2}\bar{1}1)$, $\underline{10} = (2\bar{1}1)$, $\underline{11} = (\bar{1}\bar{2}1)$, $\underline{12} = (1\bar{2}1)$. To avoid confusions between {110} and {112} slip systems, the numbers representing the slip planes are underlined.

reactions. As they were discussed in the previous parts they are not recalled here.

5.1. Major results

- The value of the Poisson ratio affects to various extents all the strengthening coefficients. In FCC metals, some coefficients substantially increase with increasing Poisson's ratio. In consequence, previously measured values are all the more affected as the Poisson ratio used in the present study differs from the previous ones.
- The double degeneracy of some coefficients has a purely geometric origin; the junction configurations are asymmetric and their strengths differ when the primary and forest slip systems are exchanged. In FCC metals, only the glissile junctions are doubly degenerated.

The computed values for germanium are in reasonable agreement with the only available experimental values on this effect [16].

- The Lomer lock is always stronger than the glissile junctions. This is the only change in the hierarchy of strengths with respect to two previous investigations in copper [7,9].
- In addition to $a/2<111>\{110\}$ slip, and to comply with current modelling, $a/2<111>\{112\}$ composite {110} slip was taken as a substitute for other composite slip systems in BCC metals. The validity of this assumption has to be further assessed.
- With respect to FCC crystals, two additional features affect the strengthening coefficients. First, the more complex slip geometry results in a multiplicity of different reactions. Second, the Burgers vector of the $a<001>$ junction is larger than that of the parent segments, which reduces the stability of junctions. For example, there are twelve junctions, of which seven are doubly degenerated. In particular, the five junctions formed by the mutual interactions of the two different {110} and {112} slip systems are all degenerated. Their strengths range from that of the Hirth lock to that of the stronger glissile junction in FCC metals. A reaction between two different slip systems leading to the formation of a degenerate junction was first observed for basal and prismatic slip in HCP ice [14].
- Save for a few exceptions, the effect of the Poisson's ratio is more marked in BCC metals than in FCC metals, especially for the junctions.
- Finally, the present work considerably extends the number of FCC and BCC materials in which strengthening coefficients were determined.

5.2. Prospective

- In the model DD simulations carried out so far, the forest is immobilized by a null Schmid factor, whereas in simulations of plastic flow all dislocation segments bow out and several slip systems may be active. Actually, when both types of simulations were carried out on FCC crystals no difference was found between the coefficient values (B. Devincre, unpublished results). Such tests will be carried out again.
- Ternary junctions, that is junctions made on pre-existing junction lines, are formed when more than two slip systems are simultaneously active. They are of minor importance in FCC crystals; it is not so in BCC crystals [38] and their values should be revisited.
- Taking into account the 'Poisson effect' and junction asymmetry effects should bring a substantial improvement to modelling. In particular the elaboration of storage-recovery models for BCC metals, especially α-iron, is a challenging task of prime importance.

Acknowledgements

R. Madec gratefully acknowledges Dr. Y.-P. Pellegrini for his early suggestion to verify whether or not the matrix of strengthening coefficients is fully symmetric. The technical assistance from Mr. M. Maglorius and Dr. L. Colombet on optimizing parallelism in the MobiDiC code is greatly appreciated.

References

[1] J. Gil Sevillano, Flow stress and work hardening, in: H. Mughrabi (Ed.), Plastic Deformation and Fracture of Metals, VCH, Weinheim, Germany, 1993, pp. 19–88.
[2] L.P. Kubin, in: A.P. Sutton, R.E. Rudd (Eds.), Dislocations, Mesoscale Simulations and Plastic Flow, Oxford Series on Materials Modelling, Oxford University Press, Oxford, 2013.
[3] P. Franciosi, M. Berveiller, A. Zaoui, Latent hardening in copper and aluminium single crystals, Acta Metall. 28 (1980) 273–283.
[4] U.F. Kocks, Laws for work-hardening and low-temperature creep, J. Eng. Mater. Eng. Technol. 98 (1976) 76–85.
[5] C. Teodosiu, J.-L. Raphanel, C. Tabourot, Finite element simulation of the large elastoplastic deformation of multicrystals, in: C. Teodosiu, J.-L. Raphanel, F. Sidoroff (Eds.), Large Plastic Deformations, AA Balkema, Rotterdam, 1993, pp. 153–168.
[6] B. Devincre, T. Hoc, L. Kubin, Dislocation mean free paths and the strain hardening of crystals, Science 320 (2008) 1745–1748.
[7] L. Kubin, B. Devincre, T. Hoc, Modeling dislocation storage rates and mean free paths in in face-centered cubic crystals, Acta Mater 56 (2008) 6040–6049.
[8] R. Madec, B. Devincre, L.P. Kubin, T. Hoc, D. Rodney, The role of collinear interaction in dislocation-induced hardening, Science 301 (2003) 1879–1882.
[9] B. Devincre, L. Kubin, T. Hoc, Physical analyses of crystal plasticity by DD simulations, Scr. Mater 54 (2006) 741–746.
[10] A. Alankar, I.N. Mastorakos, D.P. Field, H.J. Zbib, Determination of dislocation interaction strengths using discrete dislocation dynamics of curved simulations, J. Eng. Mat. Technol. 134 (2012), 021018(1-4).
[11] N. Bertin, C.N. Tomé, I.J. Beyerlein, M.R. Barnett, L. Capolungo, On the strength of dislocation interactions and their effect on latent hardening un pure magnesium, Int. J. Plast. 62 (2014) 72–92.
[12] R. Madec, L.P. Kubin, Dislocation dynamics in BCC metals: interaction strengths in the athermal regime, in: P. Vincenzini, A. Lami (Eds.), 3rd International Conference on Computational Modeling and Simulation of Materials, Part A, 2004, pp. 671–680. Techna Group Srl, Faenza, 2004.
[13] S. Queyreau, G. Monnet, B. Devincre, Slip systems interactions in α-iron determined by dislocation dynamics simulations, Int. J. Plast. 25 (2009) 361–377.
[14] B. Devincre, Dislocation dynamics simulations of slip systems interactions and forest strengthening in ice crystals, Philos. Mag. 93 (2013) 235–246.
[15] J. Amodeo, B. Devincre, Ph Carrez, P. Cordier, Dislocation reactions, plastic anisotropy and forest strengthening in MgO at high temperature, Mech. Mater 71 (2014) 62–73.
[16] H. Alexander, J.L. Crawford, Latent hardening of germanium crystals, Phys. Stat. Sol. (b) 222 (2000) 41–49.
[17] T.-Y. Wu, J.L. Bassani, C. Laird, Latent hardening in single crystals I. Theory and experiment, Proc. R. Soc. Lond. A 435 (1991) 1–19.
[18] R. Madec, B. Devincre, L.P. Kubin, From dislocation junctions to forest hardening, Phys. Rev. Lett. 89 (255508) (2002) 1–4.
[19] S.J. Basinski, Z.S. Basinski, Plastic deformation and work hardening, in: F.R.N. Nabarro (Ed.), Dislocations in Metallurgy, Dislocations in Solids, vol. 4, 1979, pp. 261–362. North-Holland, Amsterdam.
[20] S. Aubry, S.P. Fitzgerald, S.L. Dudarev, W. Cai, Equilibrium shape of dislocation shear loops in anisotropic α-Fe, Model. Simul. Mater. Sci. Eng. 19 (2011), 065006(1-14).
[21] B. Devincre, et al., Modeling crystal plasticity with dislocation dynamics simulations: the 'microMegas' code, in: O. Thomas, A. Ponchet, S. Forest (Eds.), Mechanics of Nano-objects, Presses des Mines, Paris, 2011, pp. 81–89.
[22] L. Dupuy, M. Fivel, A study of dislocation junctions in FCC metals by an orientation dependent line tension model, Acta Mater. 50 (2002) 4873–4885.
[23] R. Madec, B. Devincre, L.P. Kubin, On the use of periodic boundary conditions in dislocation dynamics simulations, in: H. Kitagawa, Y. Shibutani (Eds.), Dynamics of Fracture Process and Materials Strength (IUTAM Symposium), Kluwer, Dordrecht, 2004, pp. 35–44.

[24] L.P. Kubin, R. Madec, B. Devincre, Dislocation intersections and reactions in FCC and bcc crystals, in: H.M. Zbib, et al. (Eds.), Multiscale Phenomena in Materials, MRS Proceedings, vol. 779, MRS, Warrendale PA, 2003, pp. 25–36.
[25] R. Madec, L.P. Kubin, Dislocations interactions and symmetries in BCC crystals, in: H. Kitagawa, Y. Shibutani (Eds.), Dynamics of Fracture Process and Materials Strength (IUTAM Symposium), Kluwer, Dordrecht, 2004, pp. 69–78.
[26] W. Püschl, Reactions between glide dislocations and forest dislocations in anisotropic bcc metals, Phys. Stat. Sol. (a) 90 (1985) 181–189.
[27] L.K. Wickham, K.W. Schwarz, J.S. Stölken, Rules for forest interactions between dislocations, Phys. Rev. Lett. 83 (1999) 4574–4577.
[28] G.I. Taylor, C.F. Elam, The distortion of iron crystals, Proc. R. Soc. Lond. (A) 112 (1926) 337–361.
[29] V. Novák, B. Šesták, N. Zárubová, Plasticity of high purity iron single crystals (II) surface observations, Cryst. Res. Technol. 19 (1984) 793–807.
[30] J. Richter, The influence of temperature on slip behaviour of molybdenum single crystals deformed in tension in the range from 293 to to 573 K. II. Slip geometry and structure of slip bands, Phys. Stat. Sol. (b) 46 (1971) 203–215.
[31] N.K. Chen, R. Maddin, Slip planes and the energy of dislocations in a body-centered cubic structure, Acta Metall. 2 (1954) 49–51.
[32] K. Kitayama, et al., A crystallographic dislocation model for describing hardening of polycrystals during strain path changes. Application to low carbon steels, Int. J. Plast. 46 (2013) 54–69.
[33] B. Peeters, et al., Work-hardening/softening behaviour of B.C.C. polycrystals during changing strain paths: I. An integrated model based on substructure and texture evolution, and its prediction of the stress-strain behaviour of an IF steel during two-stage strain paths, Acta Mater 49 (2001) 1607–1619.
[34] T. Hoc, S. Forest, Polycrystal modeling of IF-TI steel under complex loading path, Int. J. Plast. 17 (2001) 65–85.
[35] E. Schmid, W. Boas, Plasticity of Crystals, F.A. Hughes & Co., Ltd., London, 1950.
[36] C.N. Reid, A review of mechanical twinning in body-centred cubic metals and its relation to brittle fracture, J. Less-Common Met. 9 (1965) 105–122.
[37] C.N. Reid, A. Gilbert, G.T. Hahn, Twinning, slip and catastrophic flow in niobium, Acta Metall. 14 (1966) 975–983.
[38] R. Madec, L.P. Kubin, Second-order junctions and strain hardening in bcc and fcc crystals, Scr. Mater. 58 (2008) 767–770.